Violin plot data: A concerto of crucial information on valve thrombogenicity classified using laboratory measured valve motion

Lawrence N. SCOTTEN[1], David BLUNDON[2], Marcus-André DEUTSCH[3], Rolland SIEGEL[4]

Affiliations:
[1] Independent consultant, Victoria, BC, Canada
[2] Instructor, Environmental Biology, Camosun College, Victoria, BC, Canada
[3] Surgeon – Cardiothoracic, Klinik fur Thorax- und Kardiovaskularchirurgie, Herz- und Diabeteszentrum NRW, Bad Oeynhausen, Germany
[4] Independent consultant, Portland, Oregon, USA

Correspondence to: Lawrence N. SCOTTEN. Dipl. T., Independent Consultant, 1560 Bonair Place, Victoria, BC V8P 4V4, Canada. Email: larryscotten2@hotmail.com

Background
We previously tested several clinical and prototype valves and observed regional flow velocities (RFV) at levels which may be related to a dimensionless thrombogenic potential (TP).

Abstract:
Objectives
This in vitro study compares mechanical (MHV) and bioprosthetic (BHV) heart valves for high amplitude short duration regional flow velocities (RFV) near valve closure.

Background
We previously tested several clinical and prototype valves and observed RFV at levels which may be related to a dimensionless thrombogenic potential (TP).
Methods
A total of four valves were tested in aortic and mitral sites under pulsatile circulation in a pulse duplicator. Valves included both clinical models and experimental prototypes. An optical approach measuring projected dynamic valve area (PDVA) to gauge valve motion was implemented. Pulsatile pressures and flow rates were measured by conventional techniques and a quasi-steady flow tester was used to measure valve leakage. RFV was derived using time-dependent volumetric flow rate/PDVA. Since flow velocity and fluid shear force are related through flow velocity gradient, TPs for valves that achieve near closure during the forward flow deceleration phase were determined as RFVs relative to the control mechanical valve RFV value of -126 m/s.
Results
TP is dimensionless and ranged between -0.45 and +1.0. Negative TPs arise when transient rebound of valve occluders is accompanied by water-hammer phenomena. Positive TPs occur during decelerating forward flow. Bioprostheses had lowest TP transient of 0.15. A mock-transcatheter aortic valve (mTAVI) incorporating by design a trivial perivalvular leak (~1.35 ml/s). demonstrated a high transient TP of 0.95.

Conclusions
Our data reveals distinct TP profile differences between valve models. If verifiable, the design of future valves may utilize currently available experimental tools to determine TPs resulting in advanced devices with significantly reduced TP.

Ultramini-Abstract
This in vitro study compares mechanical (MHV) and bioprosthetic (BHV) heart valves for high amplitude short duration inferred regional flow velocities (RFV) near valve closure.

I. Introduction and Background

Nearly 60 years after their introduction, modifications to mechanical and bioptosthetic valves have not yet resolved chronic shortcomings related to durability and thrombogenic potential. Early published data on sources of thrombogenicity in mechanical valves by Davey [1] in 1966, visualized cyclic flow behavior by high-speed cinematography in a pulse duplicator with a transparent chamber and a sheet of light flow technique using aluminum flow tracer particles in transparent test fluids. Flow patterns adjacent to an early model Starr-Edwards valve ball occluder were identified and multiple retrograde impulses were observed at valve closure. Although the investigators speculated that these events were associated with high shear, equipment of that era was incapable of measuring the retrograde flow velocities associated with occluder rebound phenomena [Davey, TB]. More recently, computational methods employed to examine flow patterns, flow velocities, and pressures associated with contemporary mechanical and bioprosthetic valve function have generated extensive information on flow but as yet have not proposed a development pathway to eliminate thrombogenicity in the former and extend durability in the latter [e.g. 2-4].

In prior publications, [5-9] we hypothesized that mechanical valve occluder closing behavior was implicated in the thrombogenic discrepancy between mechanical and bioprosthetic valves. Our modified pulse duplicator allowed measurement of prosthetic valve dynamic area (PDVA) providing crucial insight into occluder forward flow flutter, cavitation and occluder rebound that contribute to the complex genesis of valve thrombosis. Subsequent pulse duplicator adaptations included a unique electro-optical subsystem referred to as Leonardo [6] that revealed spatially averaged flow velocity in immediate proximity to test valves. We found that transient RFVs occurred often near MHV closure and proposed it as a proxy [6-9] for rapidly changing shear forces known to promote formation of micro-thrombi aggregates that may remain locally adherent or embolize. This work provided stimulation to define geometry for a mechanical heart valve (MHV) with blood damage potential reduced to tissue valve levels and this experimental methodology was extended to study thrombogenic potential in transcatheter aortic valve replacement (TAVR) devices [8, 9].

II. Methods

A) Test Apparatus

An extensively cited commercial in vitro test system [3, 5-9] was used with typical simulation conditions including pulse rate 70 beats/min; pressures ca.120/80 mmHg; and cardiac output 5 litres/min. Basic test methodology is depicted in Figure 1. Test valves included: CLINICAL MECHANICAL St. Jude Medical,

Regent™ (SJM); RAPID PROTOTYPE MECHANICAL (BV3D); CONTROL BIOPROSTHESES Edwards-Perimount and mock-TAVI construct using Edwards-Perimount valve. Nominal valve sizes were 25 mm TAD (tissue annulus diameter). Valves were tested in pulsatile and quasi-steady pressure/flow systems and PDVA profiles in pulsatile flow were obtained. Time-dependent inferred RFV was derived by dividing the volumetric flow rate by the PDVA (volumetric flow rate/PDVA). A separate leakage tester (ViVitro Labs Inc., model LT8991) provided accurate measurement of small closed valve leakage rates under quasi-steady gravity head generated pressure/flow conditions. Such measures were used to estimate aggregate valve leakage area described previously [8].

The Leonardo modified pulse duplicator originally adapted in 2011 with innovative features to measure PDVA from backlit valves remains in current use with improved spatial and temporal resolution capability (i.e., 0.001 cm^2 and 1μs). Valve data from this system was recently compared to numerical simulations for contemporary porcine tissue and bovine pericardial bioprosthetic heart valves and also with data from a similar independent pulse duplicator with excellent conformity [3].

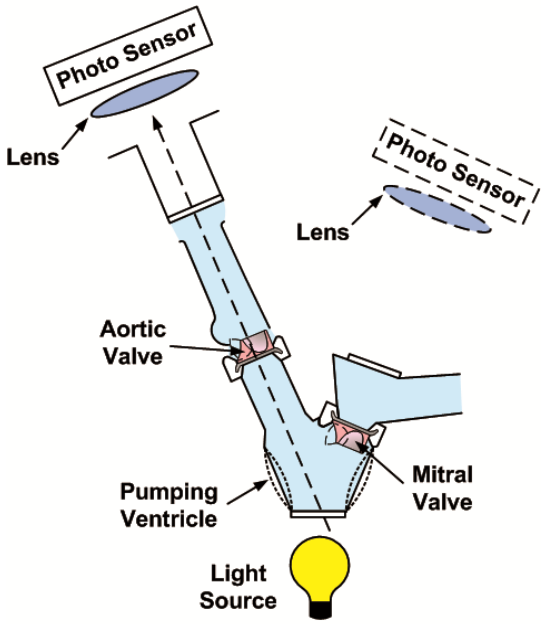

Figure 1: Optical approach gauges aortic (or mitral) prosthetic heart valve function with occluder motion quantified as projected dynamic valve area (PDVA).

A Visco-elastic Impedance Adapter (VIA) that models bulk ventricular visco-elasticity to produce physiological isovolumetric functionality has been utilized in several previous studies [3, 6-9]. Jennings et al. [10] in their use of the Leeds in vitro valve tester to study stentless porcine valves found VIA advantageous in ameliorating unphysiological left ventricular pressure oscillations. Ventricular visco-elasticity associates with valve opening and closure dynamics, ventricular pressure rates (*dp/dt*), propensity for microbubbles, high intensity trancranial signals (HITS), cavitation, acoustic emissions, and vortex flow formations. Recently, Lee et al. [3] characterized VIA as a three-element Windkessel and

utilized in fluid-structure interaction models of bioprosthetic heart valve dynamics. These models were validated with an experimental pulse duplicator.
As previously described, closed valve leakage was accurately measured in a quasi-steady pressure/flow apparatus calibrated with known small orifice areas [6-9]. Total valve leakage area was then edited into the experimental data and subsequently analyzed (leakage areas: SJM=0.0178 cm^2; BV3D=0.003 cm^2; Edwards Perimount^{TM} Bioprosthesis=0.012 cm^2).

B) Leonardo

Since only fleeting glimpses of prosthetic valve motion can be seen by the unaided eye, we developed a simple technique to quantify high speed valve motion detail (Leonardo, Figure 1). Described previously, this approach provides important analog data about valve motion [3, 5-9].

C) Regional Flow Velocity and Shear Force

Regional flow velocity magnitude shown in Figure 3 can be considered a shear force surrogate associated with valve TP. Since flow velocity and fluid shear are related through flow velocity gradient, *a proxy for valve thrombogenic potential may be inferred by flow velocity*. Although TP cannot be assumed to increase linearly with flow velocity it is considered proportional to the inferred regional flow velocity (m/s) and independent of valve fabrication materials. The regional flow velocity determined by Leonardo is an estimated spatial average quantity (m/s) and not a site specific quantity. Since flow velocity gradients cannot be obtained with Leonardo, neither can shear force values (dyne/cm^2) from measured RBVs (m/s).

D) Specifications [7]

- Temporal resolution (based on voltage step waveform response, rise time from 10% to 90% amplitude) ≈1.04 μs;
- Bandwidth ≈ 0.35/risetime = 0.35/1.04μs = 337 KHz;
- Spatial area resolution (closed valve), 0.001 cm^2 (n=10 cycle average);
- Telecentric lens maintains constant magnification ≈0.16 x;
- Working distance ≈18 cm (AORTIC); ≈19 cm (MITRAL);
- Perspective error <0.3% (depth 15 mm);
- Spatial sensitivity variation <6%;
- Typical site dependent linear regression calibrations are:
  $y=0.00128x$, with R^2 =0.99988 (AORTIC);
  $y=0.00132x$, with R^2 =0.99959 (MITRAL);
- LED back light source (diffuse red):
  Wavelength 625±15 nm
  Uniformity 99.24%
  Luminance 5,780 cd/m^2

E) Derivations and PDVA Synchronization Adjustment

Valve regional flow velocity (RFV) is equal to volumetric flow rate, divided by the PDVA (flow rate/PDVA) and is an estimate of the regional instantaneous spatial average. Regional flow velocity magnitude shown in Figure 3 can be considered a shear force surrogate associated with valve TP. Since

flow velocity and fluid shear are related through flow velocity gradient, *a proxy for valve thrombogenic potential may be inferred by flow velocity*. Although TP cannot be assumed to increase linearly with flow velocity it is considered proportional to the inferred regional flow velocity (m/s) and independent of fabrication materials. The regional flow velocity determined by Leonardo must be appreciated as an estimated spatial average quantity (m/s) and not a site specific quantity. Since flow velocity gradients cannot be obtained with Leonardo, neither can shear force values (dyne/cm^2) from measured RBVs (m/s). Valve regional flow velocity (RFV) is equal to volumetric flow rate, divided by the PDVA (flow rate/PDVA) and is an estimate of the regional instantaneous spatial average.

F) Derivations and PDVA Synchronization Adjustment

Analog signal bandwidth differences between PDVA and transvalvular volumetric flow rate were 0-337 KHz *vs.* 0-100 Hz, respectively. The PDVA signal preceded the other signals by -2.5 ms based on step signal response thus a phase adjustment between the PDVA and the other signals was required. Accordingly, post experiment, we shifted the acquired PDVA signal 1 data acquisition interval of -3.4 ms [7].

G) Violin Plots with Relative Flow Velocity Scaling

Although "Violin" plots have not previously been utilized for presentation of in vitro valve test results, they attracted our attention as a powerful graphic technique to present voluminous quantitative or qualitative data. Sample Figure 2 depicts TP data density near valve closure and reveals different peaks, their position, and relative amplitudes. Here, split-violin plots benefit from superior spatial efficiency compared to full violin plots.

The broader split-violin region(s) convey greater recurrence of TP data values whereas narrower regions(s) contain fewer recurrences. TPs for valves during the forward flow deceleration phase on the verge of closure were determined as RFVs relative to a control mechanical valve RFV value of -126 m/s. RFV was derived using time-dependent volumetric flow rate/PDVA. Since flow velocity and fluid shear force are related through flow velocity gradient, TP of valves may be a useful surrogate for transfer of shear forces to blood cells and for coagulation activation potential.

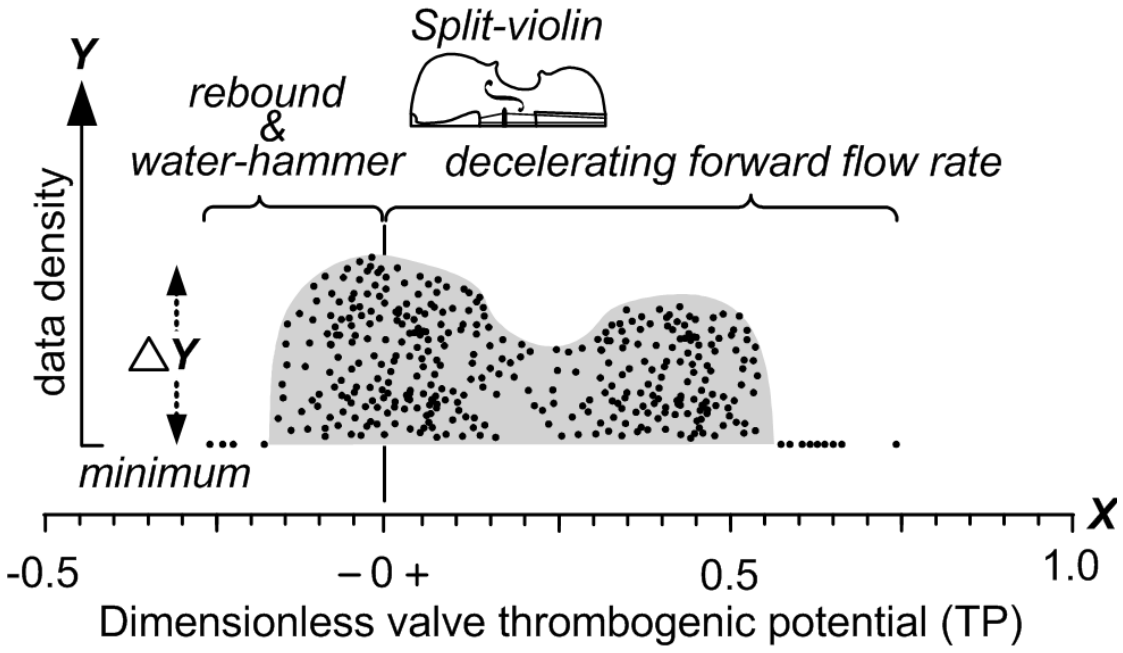

Figure 2: Sample split-violin plot depiction of inferred dimensionless valve thrombogenic potential (TP). Shaded margin ΔY represents probability of recurrence of an inferred TP (relative to an RFV of -126 m/s). All data points can be reduced to a split-violin shape with each configuration representing an independent data set and coverage of all data points for each valve and site (n=150). Single data points with minimum density depict baseline data values.

H) Valve thrombogenic potential is consistent by multiple determinations

Since 2011, our investigations utilizing Leonardo have compared TP of test valves to controls. Over time, alternate metrics for assessing TP evolved (Table I). For example, a widely used clinical MHV (SJM) has consistently exhibited high TP compared with controls regardless of determination method [6-9]. Figure 3 shows that the inferred TP for the SJM aortic valve is high (1.0) for all the determination methods listed in Table I. All determinations utilized valve motion as a component metric for obtaining TP [6-9].

Table I: Determination of TP for SJM aortic test valve -example.

Thrombogenic Potential (TP)	Quantity	References
Peak Backflow Velocity, m/s	-235	5
Thrombogenic Potential Index, TPI	3.9	7
Split violin, maximum TP	1.0	(Present study)

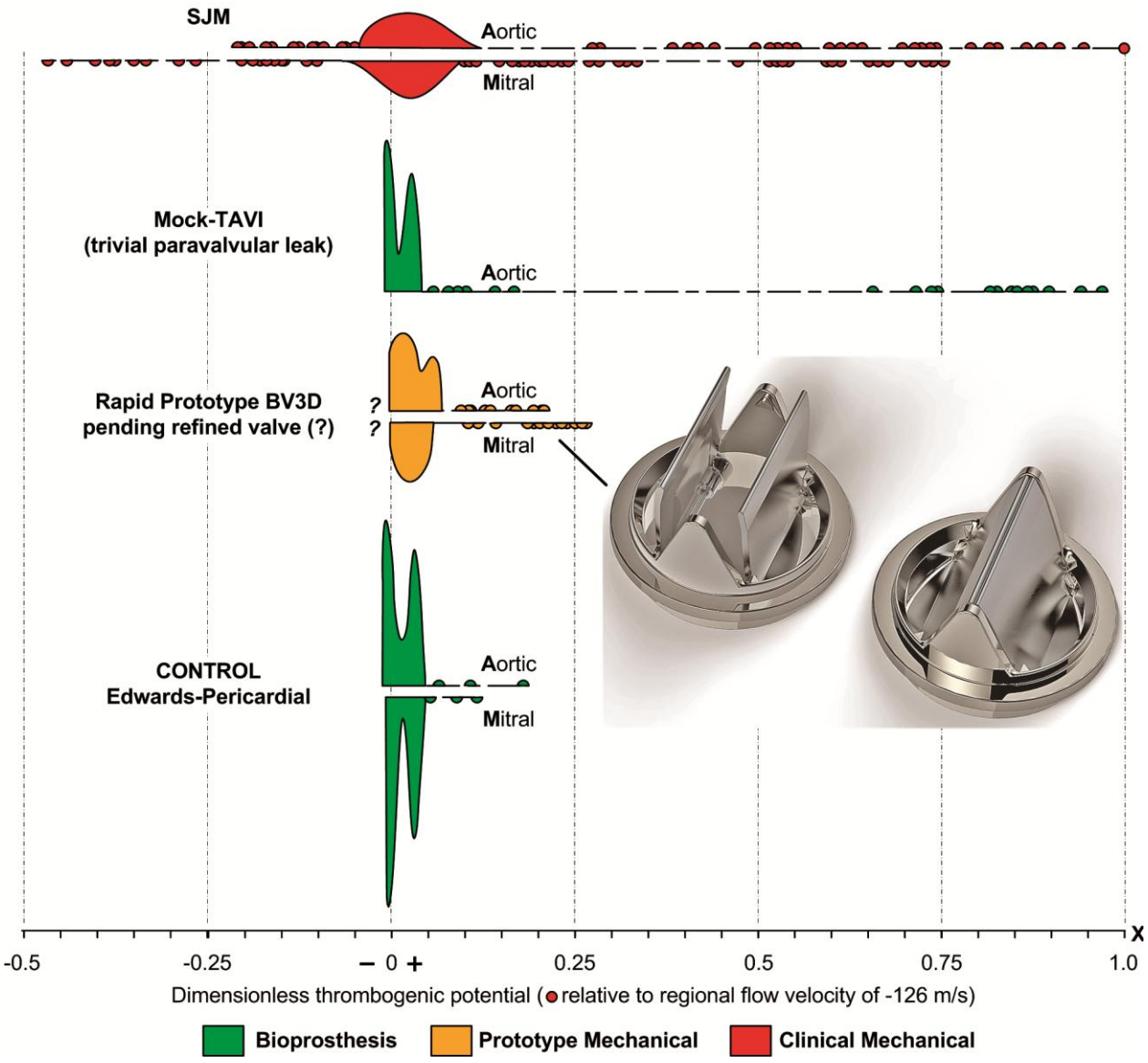

Figure 3: Inferred dimensionless TP of valves (based on near closure RFVs relative to -126 m/s). Illustrated valve BV3D shown in full open and closed positions. Negative data includes water hammer phenomena and occluder rebound RFVs except for valve BV3D. This early prototype valve is currently pending fabrication using refined prototype materials and geometry. Over the valve closing period (~495 ms, milliseconds), a total of 150 RFV data points for each of 10 consecutive cycles were acquired per experiment. Vioplot R software analyzed 10,500 data values to create full-violin plots. Subsequently, Visio software was used to trace, scale, and cut-in-half the full violin plots produced by Vioplot R to create the split-violin plots shown here.

Vioplot R* software package and Visio 2002 ** have been utilized to create the split-violin plots used in this study. Observers will appreciate that wider violin shape regions demonstrate show more probable flow velocities than those in the narrower zones.

*R Core Team (2019) R: A language and environment for statistical computing. R Foundation for Statistical Computing, Vienna, Austria. URL https://www.R-project.org/
** Microsoft, Redmond, WA USA

III. Results and Discussion

The photograph in Fig 4 from our 2011 publication [6] captures saline jetting through small clearances intrinsic to a closed SJM mechanical aortic valve driven by a transvalvular back pressure of 120 mmHg. Complex geometric gaps are present in all current mechanical valve designs. The total aggregate gap area for the closed SJM valve in Figure 4 is 0.0178 cm^2 and under pulsatile flow conditions has a maximum spatially averaged regional flow velocity of 126 m/sec near valve closure. Readers are familiar with the qualitative echocardiographic signature of these retrograde jets during immediate post implant assessment of mechanical valves to detect peri-prosthetic leak but not their magnitude and short duration of the flow transients which cannot be resolved. However, in the absence of clinically significant hemolysis, thrombotic obstruction or thromboembolic events, the longer term implications of the observed striking retrograde velocities for recipient coagulation system components have thus far remained largely unknown. With recent clinical findings that para-valvular leaks (PVL) are more common after TAVI (41-94%) then previously reported the recognition of micro-jets as a cause for hemolysis with thrombogenic consequences is now evolving [11, 12]. Interestingly, LDH values have been largely ignored until recently when a reduction of 400 U/L was reported and considered significant [11, 12]. Evidence is emerging that the smaller the leak, the higher the thrombogenic potential [8, 13].

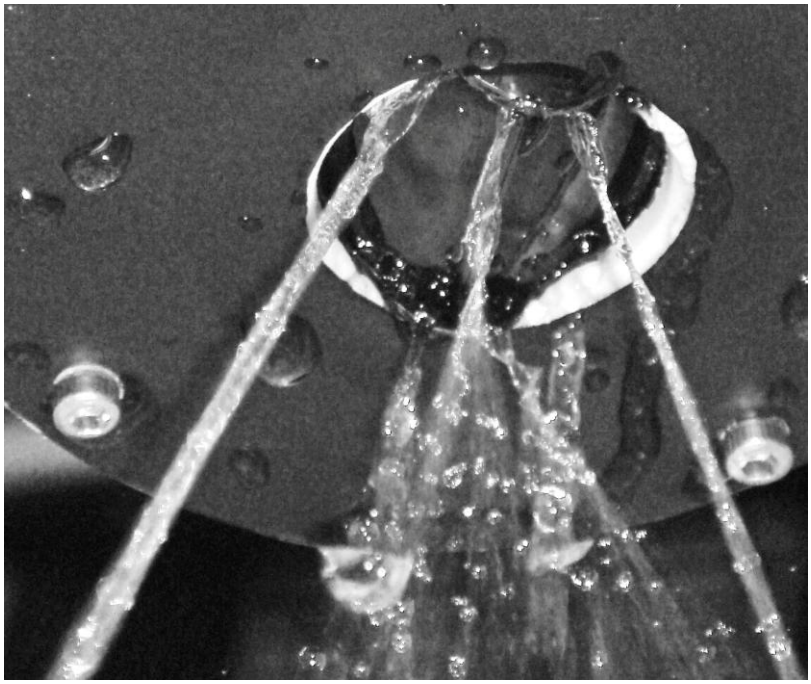

Figure 4: Photograph of retrograde jets of saline leakage passing through a closed SJM, mechanical valve TAD size 25 mm. Transvalvular backpressure on closed valve is ca. 120 mmHg. Photo details: Camera SONY model DSC-T100, f/4.4, exposure time 1/50 s, and flash mode enabled.

PVL closure may have a therapeutic effect on the extent of hemolysis that some patients experience after valve surgery. Reduction of hemolysis is most likely in a patient with a mechanical valve and is not necessarily correlated with the volume of regurgitant flow or its subsequent reduction. Hemolysis associated with biological valves are less likely to respond to peri-valvular leak closure suggesting that mechanisms other than net volume of regurgitation or micro-jets are present and should be considered [11,12].

Near valve closure, flow dynamics can be considered analogous to transient valve stenosis, whereby regurgitation is increasingly constrained until complete motionless closed valve condition occurs. During brief crucial moments preceding valve closure, localized prothrombotic microenvironments may be relevant to generation of high velocity leakage jets, flow unsteadiness, valve flutter, cyclic variability of PDVA, turbulence, and excessive shear forces that may induce blood element damage [15-29]. These influences may impact multiple valve types for:

- conduction abnormalities
- reduced mobility of valve leaflets or occluders [29]
- silent cerebral micro-infarction [17, 22-25]
- sub-clinical valve thrombosis [18, 25-27]
- potential for pannus formation
- acute and sub-acute embolic stroke and other adverse cerebrovascular events including TIA [17-19]
- cavitation and high intensity trans-cranial signals (HITS) [6]

Closure dynamics therefore raise provocative questions about valve thrombogenic impact including:

1. Dynamics of valve closure that may mimic well studied pro-thrombotic aspects of forward valve flow (e.g., valve stenosis) and arterial flows (e.g., arterial sclerosis)
2. Valve closure dynamics may reflect combined biomechanical and biochemical responses sufficient to exacerbate risk for pathologic thrombus formation and propagation
3. Valve rebound and water-hammer -the SJM valve in the mitral position consistently manifested leaflet rebound observed as a momentary post closure partial re-opening driven by water-hammer power (transvalvular pressure × volumetric flow rate). This has been previously reported with magnified examples of high-resolution PDVA rebound data [7].

Figure 3 compares several contemporary and prototype cardiac valves near closure extending over the ~495 ms each cycle of 10 consecutive cycles gathered. One hundred fifty (150) RFV data points were collected for every cycle and 10 consecutive cycles were collected for each valve. The time increment was ~3.4 ms which was the interval used to collect data over the total cycle time of 867 ms (cycle rate =70 per minute). Inferred dimensionless TP of the test valves (X axis) is referenced to an RFV of -126 m/s, the peak observed for the SJM aortic MHV.

A) Study outcomes (previous and present reports) [6-9]:

1. High amplitude RFVs and resultant supra-physiologic shear forces originating in small intra- and para-valvular leakage (PVL) gaps are mechanistic initiators of the clotting cascade.

2. Platelet activation is induced by high shear even with short exposure time [17,18]
3. The disparity in closing dynamics between MHV *vs.* bioprosthetic valves is chronically overlooked as a primary indicator of valve TP.
4. Current MHVs have overt RFV transients at closure relating to occluder non-response to flow deceleration and residual PDVA.
5. A mock TAVR valve with trivial PVL generated high magnitude short duration RFVs.
6. An unintended consequence of reducing significant PVL to trivial PVL produces high RFVs and increased valve TP.
7. For a given volumetric backflow rate near valve closure, the smaller the total residual leakage area, the greater the magnitude of RFVs.
8. The highest recorded RFVs were generated by the SJM valve compared to the tissue control valves (Edwards pericardial).
9. Rapid prototype valve BV3D produced RFVs similar to the tissue control valves.
10. A spatial average of RFVs in immediate proximity to prototype valves may be a practical indicator in qualitative screening for valve TP.
11. Test data from valve BV3D strongly suggest that specific MHV leaflet geometries generate a closure force during forward flow deceleration and prior to flow reversal, a potentially beneficial "soft closure" response.
12. Since the motion of heart valves is too fast to see and too important to ignore, Leonardo provides a simple rapid means to pre-calibrate, record, and perform quantitative valve motion analysis.
13. Our technology enabled RFVs to be resolved and focused attention on overt RFVs previously overlooked and hidden due to brevity, small PVL gaps, and limited instrumentation resolution capability.
14. Our results infer shear damage to formed blood elements and a resultant continuous thrombogenic response constitute a mechanistic explanation for observed thrombogenic disparity in prosthetic valve types and designs now broadened to include observations of TAVI related thromboembolic events.
15. For MHVs, cyclic RFVs appear to be related to a prothrombotic state requiring chronic anti-coagulation [28]. This risk is much less recognized in bioprosthetic heart valves which appear not to generate a pro-thrombotic closing phase but TAVI prostheses with trivial PVL may generate pathologic RFVs similar to those observed in MHVs.
16. Promising prototype MHVs were designed and tested *in vitro* with dimensions optimized to provide minimum TP relative to BHV controls thereby attenuating potential of hemodynamic biomechanical forces and biochemical pathways known to initiate and amplify thrombus formation.

B) Caveats

RFVs are useful surrogates for flow induced blood cell damage potential but TP cannot be directly inferred from derived maximum flow velocities considering the complexity of blood coagulation factors recently reviewed by Rana and associates [19]. For example, the difference between laminar and turbulent flow and their respective impact on blood component damage awaits experimental evidence to validate numerical simulations [20]. In contrast to laminar flow, turbulent fluid flow is characterized by chaotic flow/pressure fluctuations with sufficient shear force to activate blood clotting mechanisms and influence von Willebrand factor (vWF) mechanisms [30, 31].

IV. Conclusions

Importance – Our prior work found that valve motion and flow velocity constitute a primary contribution to valve TP and that closure-related functional deficit is a common shortcoming of current MHVs [6-9]. Progress beyond the limitations of current prosthetic valves requires appreciation of valve closure as a crucial factor since very high flow short duration RFVs near valve closure result in transient blood cell damage during each cardiac cycle and initiation of the coagulation cascade [17, 18]. Additionally, results suggest that designing a MHV with reduced TP comparable to clinically well established tissue valves is achievable with current technology. On a cautionary note, device manufacturers preoccupied with modifications of catheter delivered valves to minimize residual leak assume that a minor (trivial) leak diminishes patient risk. However, we consistently observe smaller volume-metric PVLs to associate with higher magnitude RFVs and conversely; that larger PVLs result in lower RFVs and shear forces. This is consistent with recently reported clinical experience where independent predictors of late leaflet thrombosis up to 3 years post implant were male sex *and PVL less than mild* [13]. Lastly, perhaps the most consequential outcome of our work is development of a practical method to screen experimental valves for inferred thrombotic potential compared with well established clinical controls.

Footnotes

Contributions: (I) Conception and design: LN Scotten; (II) Administrative support: LN Scotten; (III) Provision of study materials: LN Scotten; (IV) Collection and assembly of data: LN Scotten; (V) Data analysis and interpretation: LN Scotten, D Blundon; (VI) Manuscript writing: All authors; (VII) All authors have approved the final submitted version of the manuscript.

Acknowledgements: Jason Nicholls utilized SolidWorks software for modeling and Keyshot software for rendering the valve prototype BV3D in Figure 3.

Competing Interests: None declared.

Provenance and peer review: Not commissioned; externally peer reviewed

Financial Disclosure: This research has been done on a *pro bono* basis by all authors with no financial support of others.

Data sharing statement: All data relevant to the study are included in the article.

V. References

[1] Davey TB, Kaufman B, Smeloff, EA. Pulsatile flow studies of prosthetic heart valves. J Thorac Cardiovasc Surg 1966;51:264-7. Google Scholar

[2] Bluestein D, Chandran KB, Manning KB. Towards non-thrombogenic performance of blood recirculating devices. Ann Biomed Eng 2010;38:1236-56. PubMed Abstract | Google Scholar

[3] Lee JH, Rygg AD, Kolahdouz EM, Rossi S, Retta SM, Duraiswamy N, Scotten LN, Craven BA, Griffith BE. Fluid-structure interaction models of bioprosthetic heart valve dynamics in an experimental pulse duplicator. Ann Biomed Eng 2020;7 Feb 2020 https://doi.org/10.1007/s10439-020-02466-4

[4] Consolo F, Sheriff J, Gorla S, Magri N, Bluestein D, Pappalardo F, Slepian MJ, Fiore GB, Redaelli A. High frequency components of hemodynamic shear stress profiles are a major determinant of shear-mediated platelet activation in therapeutic blood recirculating devices. Sci Rep 2017;7:4994-5008. PubMed Abstract | Google Scholar

[5] Scotten LN, Walker DK. New laboratory technique measures projected dynamic area of prosthetic heart valves. J Heart Valve Dis 2004;13:120-32; discussion 132-3. PubMed Abstract | Google Scholar

[6] Scotten LN, Siegel R. Importance of shear in prosthetic valve closure dynamics. J Heart Valve Dis 2011;20:664-72. PubMed Abstract | Google Scholar

[7] Scotten LN, Siegel R. Are anticoagulant independent mechanical valves within reach –fast prototype fabrication and in vitro testing of innovative bi-leaflet valve models. Ann Transl Med 2015;3:197-205. PubMed Abstract | Google Scholar

[8] Scotten LN, Siegel R. Thrombogenic potential of transcatheter aortic valve implantation with trivial paravalvular leakage. Ann Transl Med 2014;2:43. PubMed Abstract | Google Scholar

[9] Chaux A, Grey RJ, Stuoka JC, Emkin MR, Scotten LN, Siegel R. Anticoagulant independent mechanical heart valves –viable now or still a distant holy grail. Ann Transl Med 2016;4:525-601. PubMed Abstract | Google Scholar

[10] Jennings L, Butterfield M, Walker PG, Watterson KG, Fisher J. The influence of ventricular impedance on the hydrodynamic performance of bioprosthetic aortic roots in vitro. J Heart Valve Dis 2001;10:269-275 PubMed Abstract | Google Scholar

[11] Gilchrist IC. Treating hemolysis due to paravalvular leaks: It is all about modifying micro-jets and not the volume of regurgitation. Catheter Cardiovasc Interv 2019;93:720-721. PubMed Abstract | Google Scholar

[12] Panaich SS, Maor E, Reddy G, Raphael CE, Cabalka A, Hagler DJ, Reeder GS, Rihal CS, Eleid MF. Effect of percutaneous paravalvular leak closure on hemolysis. Catheter Cardiovasc Interv 2019;93:713-719. https://doi.org/10.1002/ccd.27917 PubMed Abstract | Google Scholar

[13] Yanagisawa R, Tanaka M, Yashima F, Arai T, Jinzaki M, Shimizu H, Fukuda K, Watanabe Y, Naganuma T, Higashimori A, Mizutani K, Araki M, Tada N, Yamanaka F, Otsuka T, Yamamoto M, Hayashida K. Early and late leaflet thrombosis after transcatheter aortic valve replacements a multicenter initiative from the OCEAN-TAVI registry Circ Cardiovasc Interv 2019;12:e007349. doi: 10.1161/CIRCINTERVENTIONS. 118.007349 PubMed Abstract | Google Scholar

[14] Alizadeh M, Cote M, Albu AB. Leaflet free edge detection for the automatic analysis of prosthetic heart valve opening and closing motion patterns from high speed video recordings. Image Analysis 2017 20th Scandinavian Conference, SCIA 2017; Part II, LNCS 10270:15-27. doi: 10.1007/978-3-319-59129-2 Google Scholar

[15] Quinlan HJ, Dooley PN. Models of flow-induced loading on blood cells in laminar and turbulent flow, with application to cardiovascular device flow. Ann Biomed Eng 2007;35:1347-1356. doi:10.1007/s10439-007-9308-8 PubMed Abstract | Google Scholar

[16] Hatoum H, Yousefi A, Lilly S, Maureira P, Crestanello J, Dasi LP. An in vitro evaluation of turbulence after transcatheter aortic valve implantation. J Thorac Cardivasc Surg 2018;156:1837-1848. PubMed Abstract | Google Scholar

[17] Ding J, Chen Z, Niu S. Quantification of shear-induced platelet activation: High shear stresses for short exposure time. Artificial Organs 2015;39:576-83. PubMed Abstract | Google Scholar

[18] Soares JS, Sheriff J, Bluestein D. A novel mathematical model of activation and sensitization of platelets subjected to dynamic stress histories. Biomech Model Mechanobiol 2013;12:1127-41. doi: 10.3389/fcvm.2019.00141 PubMed Abstract | Google Scholar

[19] Rana A, Westein E, Niego B, Hagemeyer CE. Shear-dependent platelet aggregation: mechanisms and therapeutic opportunities. Front Cardiovasc Med 2019;6:141-162. doi: 10.3389/fcvm.2019.00141 PubMed Abstract | Google Scholar

[20] Faghih MM, Sharp MK. Modeling and prediction of flow-induced hemolysis: a review. Biomechanics and Modeling in Mechanobiol 2019;18:845–881. doi: 10.3389/fcvm.2019.00141 PubMed Abstract | Google Scholar

[21] Rosseel L, De Backer O, Søndergaard L. Clinical valve thrombosis and subclinical leaflet thrombosis following transcatheter aortic valve replacement: Is there a need for a patient-tailored antithrombotic therapy? Front Cardiovasc Med 2019; 6:44-54. doi: 10.3389/fcvm.2019.00044 PubMed Abstract | Google Scholar

[22] Armijo G, Nombela-Franco L, Tirado-Conte G. Cerebrovascular events after transcatheter aortic valve implantation. Front Cardiovasc Med 2018;5:104-118. doi: 10.3389/fcvm.2018.00104. PubMed Abstract | Google Scholar

[23] Musa TA, Uddin A, Loveday C, Dobson LE, Igra M, Richards F, Swoboda PP, Singh A, Garg P, Foley JRJ, Fent GJ, Goddard AJP, Malkin C, Plein S, Blackman DJ, McCann GP, Greenwood JP. Silent cerebral infarction and cognitive function following TAVI: an observational two-centre UK comparison of the first-generation CoreValve and second-generation Lotus valve. BMJ Open 2019;9:e022329 doi:10.1136/bmjopen-2018-022329 PubMed Abstract | Google Scholar

[24] Rashid HN, Gooley RP, Nerlekar N, Ihdayhid AR, McCormick LM, Nasis A, Cameron JD, Brown AJ. Bioprosthetic aortic valve leaflet thrombosis detected by multidetector computed tomography is associated with adverse cerebrovascular events: a meta-analysis of observational studies. EuroIntervention 2018; 13:e1748-55. PubMed Abstract | Google Scholar

[25] Rashid HN, Cameron JD, Brown AJ. Activation of the coagulation cascade and the role of paravalvular leak in the development of leaflet thrombosis following transcatheter aortic valve replacement. EuroIntervention 2018;14:718-719. PubMed Abstract | Google Scholar

[26] Deutsch MA, Scotten LN, Siegel R, Lange R, Bleiziffer S. Leaflet thrombosis and clinical events after TAVR: are paravalvular leaks a crucial trigger? EuroIntervention 2018;14:716-717. PubMed Abstract | Google Scholar

[27] Khodaee F, Barakat M, Abbasi M, Dvir D, Azadani AN. Incomplete expansion of transcatheter aortic valves is associated with propensity for valve thrombosis InteractCardioVasc Thorac Surg 2019; doi:10.1093/icvts/ivz213. PubMed Abstract | Google Scholar

[28] Aimo A, Giugliano RP, De Caterina R. Non-vitamin K antagonist oral anticoagulants for mechanical heart valves, is the door still open? Circulation 2018;138:1356-1365. PubMed Abstract | Google Scholar

[29] Themudo R, Kastengren M, Broloin EB, Cederlund K, Svensson A, Dalen M. Leaflet thickening and stent geometry in sutureless bioprosthetic aortic valves. Heart Vessels 2020 doi:10.1007/s00380-020-01553-9 PubMed Abstract | Google Scholar

[30] Van Belle E, Vincent F, Rauch A, Casari C, Jeanpierre E, Loobuyck V, Rosa M, Delhaye C, Spillemaeker H, Paris C, Debry N, Verdier B, Vincentelli A, Dupont A, Lenting PJ, Susen S. von Willebrand factor and management of heart valve disease. J Am Coll Cardiol 2019;73:1078-1088. PubMed Abstract | Google Scholar

[31] Van Belle E, Rauch A, Vincent F, Robin E, Kibler M, Labreuche J, Jeanpierre E, Levade M, Hurt C, Rousse N, Dally JB, Debry N, Dallongeville J, Vincentelli A, Delhaye C, Auffray JL, Juthier F, Schurtz G, Lemesle G, Caspar T, Morel O, Dumonteil N, Duhamel A, Paris C, Dupont-Prado A, Legendre P, Mouquet F, Marchant B, Hermoire S, Corseaux D, Moussa K, Manchuelle A, Bauchart JJ, Loobuyck V, Caron C, Zawadzki C, Leroy F, Bodart JC, Staels B, Goudemand J, Lenting PJ, Susen S. Von Willebrand Factor ultimers during transcatheter aortic-valve replacement N Engl J Med 2016;375:335-44. PubMed Abstract | Google Scholar